American Journal of Pathology, Vol. 138, No. 4, April 1991

Rosenthal Fibers Share Epitopes with αB-Crystallin, Glial Fibrillary Acidic Protein, and Ubiquitin, But Not with Vimentin

Immunoelectron Microscopy with Colloidal Gold

Naoyuki Tomokane,*† Toru Iwaki,*‡
Jun Tateishi,* Akiko Iwaki,‡ and
James E. Goldman‡

From the Department of Neuropathology, Neurological Institute and the Department of Orthopedics, Faculty of Medicine, Kyushu University,† Fukuoka, Japan; and the Department of Pathology, Columbia University College of Physicians and Surgeons, New York, New York‡*

Ultrastructural immunoreactivities of αB-crystallin, glial fibrillary acidic protein (GFAP), ubiquitin, and vimentin in Rosenthal fibers (RFs) isolated from an Alexander's disease brain were investigated using nonosmium and low-temperature embedding technique. The morphology of RFs embedded in Lowicryl K4M resin was well preserved after treatment with 0.5% Triton X-100. αB-crystallin immunoreactivity was present in RFs of various sizes and was the strongest in loosely scattered deposits, which were considered to be the initial stage of RFs. Glial fibrillary acidic protein immunoreactivity in RFs was heavy, homogeneous throughout RFs, and equivalent to that in networks of glial filaments. Immunoreactivities of both αB-crystallin and GFAP were mainly restricted to the high electron-dense areas within RFs and were proved to exist close to each other by double immunolabeling. Rosenthal fibers were negative for vimentin. Ubiquitin immunoreactivity was relatively homogeneous in RFs with small diameters, but in RFs with large diameters, the immunoreactivity diminished in the center. Based on these observations, combined with the tendency of self-aggregation of αB-crystallin, it is conceivable that RFs are huge aggregation products of αB-crystallin involving GFAP, and that ubiquitination may be a consequent phenomenon, as it may be in other intracytoplasmic inclusions, such as neurofibrillary tangles and Lewy bodies. (Am J Pathol 1991, 138:875–885)

Rosenthal fibers (RFs) are carrot-shaped or beaded inclusions that appear in astrocytes under certain pathologic conditions, such as Alexander's disease, glial tumors, and glial scar tissue.[1–15] Since they were first described by Rosenthal in 1898,[1] the pathogenesis or morphogenesis of RFs has remained a subject of controversy. Ultrastructurally RFs are irregular, electron-dense, and amorphous substances with distinct margins, and they are intimately related to a dense feltwork of intermediate filaments.[7–10,13–15]

Because of this association with intermediate filaments, several investigators have examined immunoreactivities of RFs with antibodies to glial fibrillary acidic protein (GFAP), the major intermediate filament protein of astrocytes. Glial fibrillary acidic protein immunoreactivity of RFs at the light-microscopic level has been observed around their periphery.[13,15–17] Recent immunoelectron-microscopic observation of RFs with anti-GFAP antibodies, however, demonstrated the presence of GFAP immunoreactivity in the amorphous, electron-dense materials of RFs.[18,19] Ubiquitin immunoreactivity has been also found to be present in RFs, mainly at their periphery.[20,21] Ubiquitin, a highly conserved protein of 76 amino acids, is thought to play a regulatory role for the nonlysosomal degradation of proteins in eukaryotic cells by forming conjugates with abnormal proteins.[22] Ubiquitin is also present in neuronal inclusions, such as the neurofibrillary

Supported by a Grant-in-Aid for General Scientific Research No. 02670154 from the Ministry of Education, Science and Culture of Japan.

Accepted for publication December 3, 1990.

Address reprint requests to N. Tomokane, MD, Department of Neuropathology, Neurological Institute, Faculty of Medicine, Kyushu University 60, 3-1-1 Maidashi, Higashiku, Fukuoka 812, Japan.

tangles of Alzheimer disease, Lewy bodies of Parkinson disease, and Pick bodies of Pick disease.[20,23]

The pathologic picture of Alexander's disease is characterized by a massive accumulation of RFs in the central nervous system associated with demyelination. Although the clinical entity of infantile cases of Alexander's disease has been established, there has been little progress in our understanding of the etiology of Alexander's disease. We have been studying the composition of RFs to try to gain insights into the pathogenesis of this disorder. We found that a RF-enriched fraction from Alexander's disease brain was composed of three major proteins: vimentin, GFAP, and αB-crystallin, a component of the vertebrate lens and now known to be expressed in extralenticular tissues.[24–27] Rosenthal fibers in several conditions, including Alexander's disease, tumors, and astrocytes in glial scar tissue show a similar immunoreaction for αB-crystallin.[17,24]

In this ultrastructural study, we investigated the immunoreactivities of αB-crystallin, GFAP, vimentin, and ubiquitin in RFs by immunoelectron microscopy using postembedding immunogold technique on ultrathin sections of extracted RFs from an Alexander's disease brain.

Materials and Methods

Rosenthal Fibers for Immunoelectron Microscopy

Crude extracts of RFs were obtained from an Alexander's disease brain by the modified procedure of Goldman and Corbin.[17] One hundred milligrams of frozen cerebral white matter was mildly homogenized with 0.5% Triton X-100, 2 mmol/l (millimolar) ethylene diamine tetraacetic acid (EDTA), 2 mmol/l phenylmethyl sulfonyl fluoride, 50 mmol/l TRIS-HCl, pH 6.8, at 10:1 buffer-to-tissue ratio (vol/wt). After centrifugation at 10,000*g* for 15 minutes, the supernatant was discarded and the pellet was fixed with 4% paraformaldehyde and 0.5% glutaraldehyde (GA) in 0.1 mol/l (molar) phosphate buffer, pH 7.4 (PB) for 2 hours with continuous agitation. After fixation, the pellet was rinsed three times in distilled water, dehydrated in gradient dimethyl formamide with intervening centrifugation and resuspension, and embedded in Lowicryl K4M (Polysciences, Warrington, PA) at 4°C according to Altman et al.[28] In a comparative experiment, formaldehyde-fixed white matter of the same patient enriched with RFs was postfixed for 2 hours at room temperature in 1% osmium tetroxide and embedded in Epon (E. Fullam, Inc., Latham, NY). Silver-colored ultrathin sections were placed on nickel grids coated with collodion and carbon (200 mesh).

Antibodies

A rabbit polyclonal anti–αB-crystallin antiserum was raised against αB-crystallin purified from rat cardiac muscle, and the specificity of the antibody to αB-crystallin was confirmed by Western blotting.[24] The antibody cross-reacts with αB-crystallin of bovine and human species. The following antibodies were also used: a rabbit polyclonal anti-human GFAP antiserum, a mouse monoclonal anti-porcine GFAP antibody (clone G-A-5), a rabbit polyclonal anti-human ubiquitin antiserum, and a mouse monoclonal anti-porcine vimentin antibody (clone V9). The monoclonal antibodies were purchased from Boehringer-Mannheim Biochem (Indianapolis, IN). Anti-ubiquitin was purchased from Sigma (St. Louis, MO). The preparations and characterizations of those antibodies previously were described.[29–32] The optimal dilutions of these antibodies were preliminarily determined as those with both maximal specific staining and minimal background staining (Table 1).

Gold Probes

For the single immunogold staining technique (IGS), we used goat anti-rabbit IgG conjugated to 15-nm colloidal gold particles (GAR-G15) or goat anti-mouse IgG conjugated to 15-nm gold (GAM-G15). For double IGS, we used goat anti-rabbit IgG conjugated to 10-nm gold (GAR-G10) and goat anti-mouse IgG conjugated to 5-nm gold (GAM-G5). Gold-labeled secondary antibodies were purchased from Janssen Biotech (Beerse, Belgium).

Immunocytochemistry

Phosphate buffer, 0.1 mol/l, supplemented with 1% bovine serum albumin and 0.3 mol/l NaCl (PBB), was

Table 1. *Characteristics and Dilutions of Antisera Used for Immunogold Labeling of RFs and Intermediate Filaments*

Antisera to	Immunized species	Source of immunogen	Dilution
αB-crystallin (polyclonal)	Rabbit	Rat cardiac muscle	250×
GFAP (polyclonal)	Rabbit	Human brain glial filament	500×
GFAP (monoclonal)	Mouse	Porcine spinal cord glial filament	50×
Ubiquitin (polyclonal)	Rabbit	Human erythrocyte	1000×
Vimentin (monoclonal)	Mouse	Porcine eye lens	50×

used for rinsing and for diluting normal goat serum, primary antibodies, and the colloidal gold reagents. With the exception of the colloidal gold, all solutions for postembedding IGS were passed through a 0.22-μ Millipore filter (Millipore, Japan) before use. For the single IGS, grids were floated with the section side down at room temperature on the following solutions:

1) distilled water for 10 minutes
2) 5% normal goat serum for 10 minutes
3) the primary antibodies overnight (dilutions are listed in Table 1.)
4) PBB for 10 minutes × 3
5) a 1:25 dilution of appropriate gold-labeled secondary antibody for 1 hour
6) PBB for 10 minutes × 3
7) 2% GA in 0.01 mol/l PBS, pH 7.4 for 10 minutes
8) distilled water for 10 minutes × 3

Sections labeled with colloidal gold were contrasted with uranyl acetate and lead citrate before examination.

To examine the distribution of both αB-crystallin and GFAP in the same section, double IGS was performed by two different procedures: simultaneous double IGS and sequential double IGS. Simultaneous double IGS was done by floating grids on a mixture of a rabbit polyclonal anti–αB-crystallin antiserum and a mouse monoclonal anti-GFAP antibody or a mouse monoclonal anti-vimentin antibody, followed by a mixture of GAR-G10 and GAM-G5. Sequential double IGS was done by repeating single IGS; single labeling first was performed without postfixation with GA, and another single-labeling procedure was carried out with the corresponding gold probe of a different size.

Morphometry

Quantitative evaluation of labeling distribution was performed by counting gold particles. A minimum of 10 electron micrographs, illustrating labeled RFs, was taken for each experiment at × 12,000 magnification and then enlarged to × 30,000. In RFs with heterogeneous electron density, distribution of gold particles on high or low electron-dense areas of each RF was investigated for reactions with anti–αB-crystallin, GFAP (with a monoclonal antibody), and ubiquitin. In addition, the number of gold particle for αB-crystallin labeling in RFs was compared for three different double immunolabeling methods using anti-GFAP as another antibody.

Controls

Specificity of the immunolabeling was tested by the following controls. (1) Incubation of sections in anti–αB-crystallin antiserum that had been absorbed with

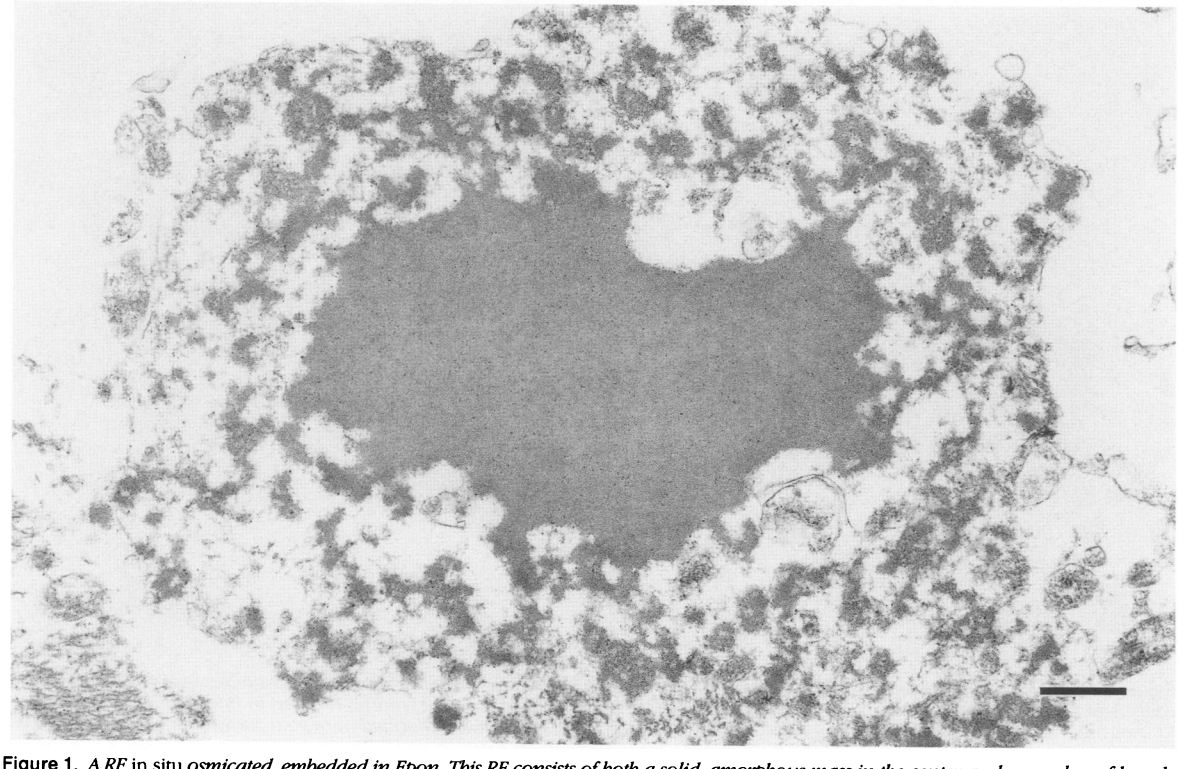

Figure 1. *A RF* in situ *osmicated, embedded in Epon. This RF consists of both a solid, amorphous mass in the center and a number of loosely scattered electron-dense deposits in the periphery. Original magnification × 24,000. Bar, 0.5 μ.*

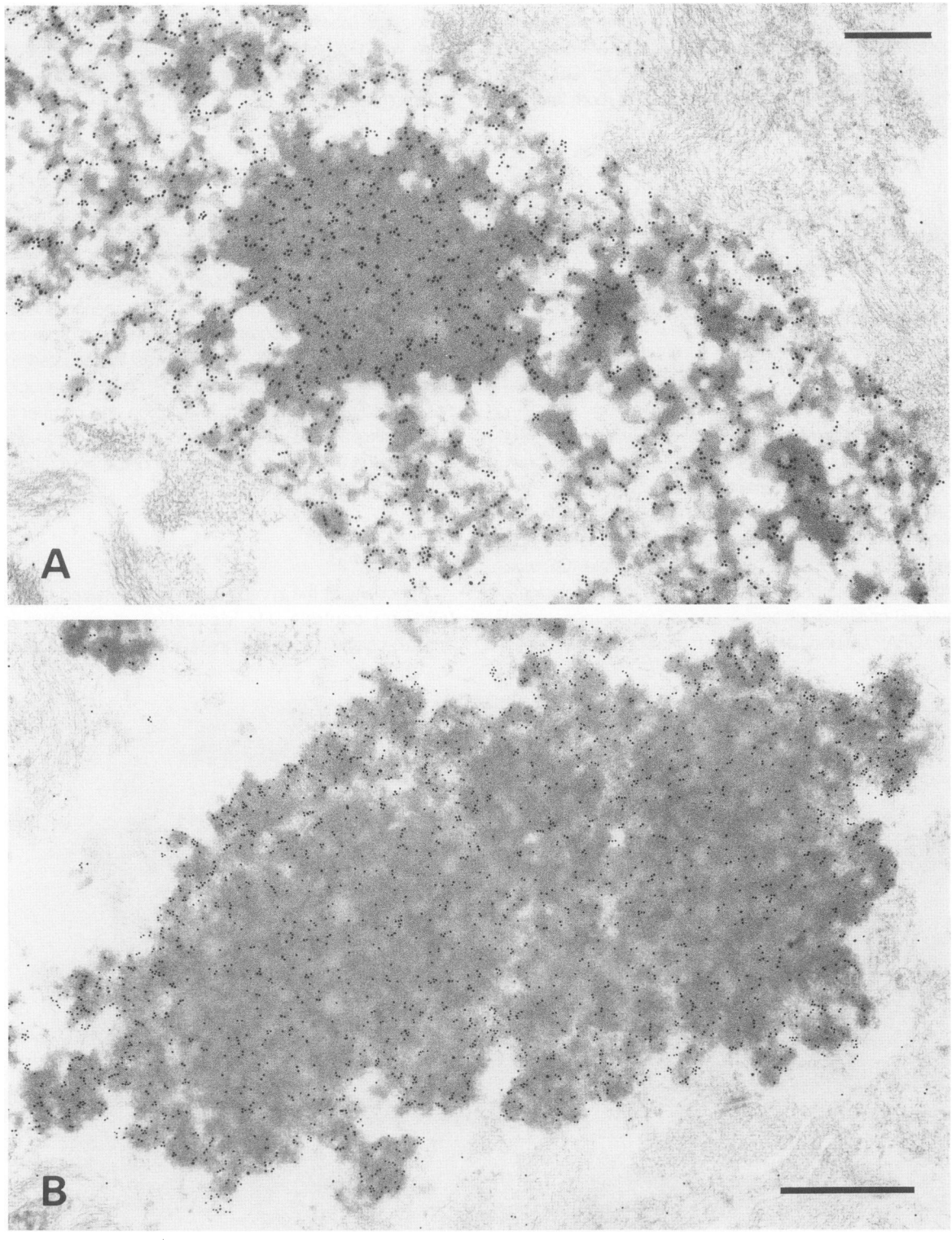

Figure 2. *Immunogold localization of αB-crystallin.* **A:** *A combined type of a RF. Immunoreactivity in the loosely scattered deposits was equivalent to or a little stronger than that in the solid mass of the center. Only a few gold particles are seen in intermediate filaments.* **B:** *A RF showing a solid mass. The RF has heterogeneous electron density. Note the favorable distribution of gold particles in high electron-dense areas. Original magnifications:* **A,** × *22,000;* **B,** × *29,000. Bars:* **A,** *0.5* μ; **B,** *1* μ.

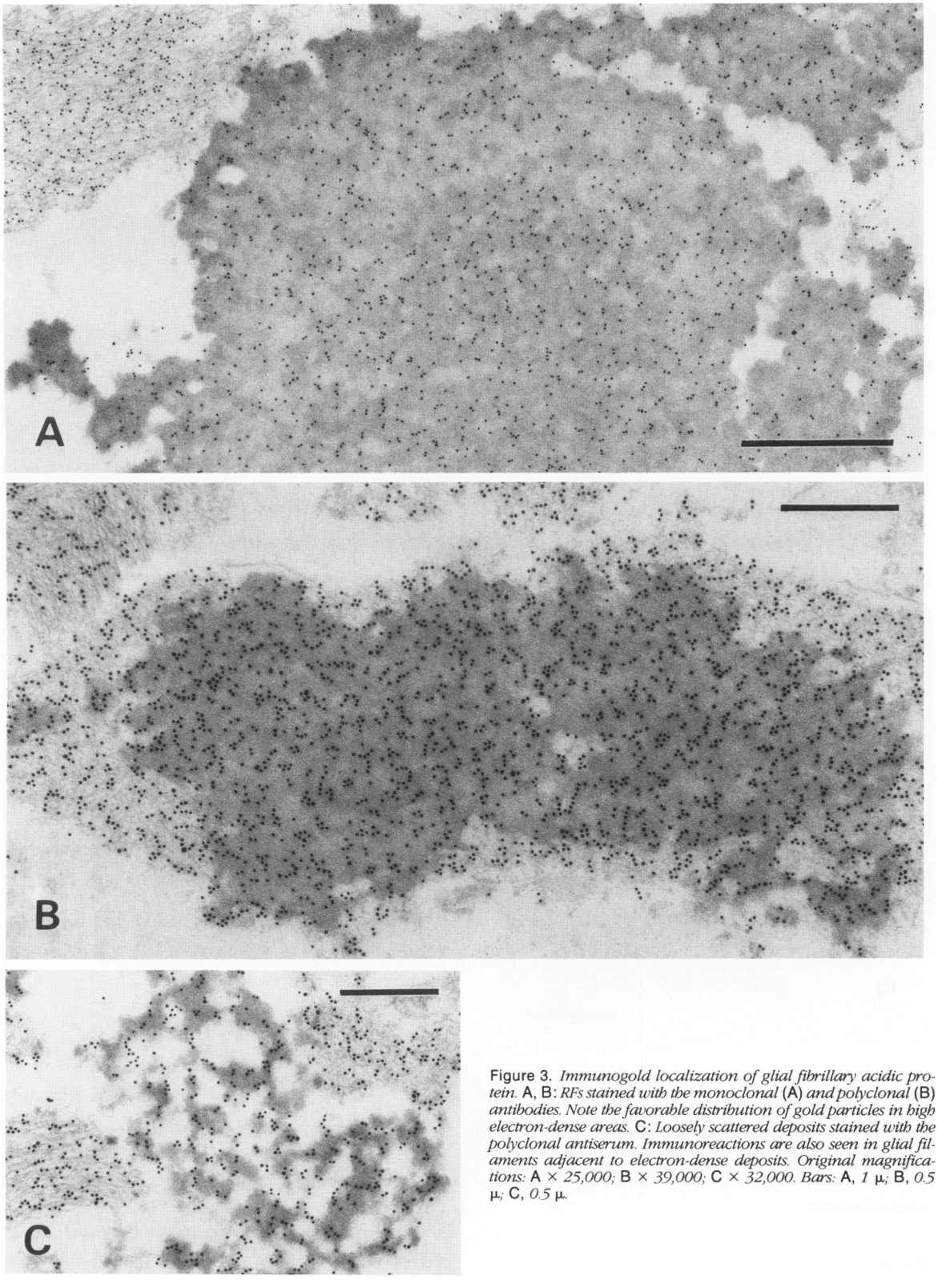

Figure 3. *Immunogold localization of glial fibrillary acidic protein.* A, B: *RFs stained with the monoclonal* (A) *and polyclonal* (B) *antibodies. Note the favorable distribution of gold particles in high electron-dense areas.* C: *Loosely scattered deposits stained with the polyclonal antiserum. Immunoreactions are also seen in glial filaments adjacent to electron-dense deposits. Original magnifications:* A × *25,000;* B × *39,000;* C × *32,000. Bars:* A, *1* μ; B, *0.5* μ; C, *0.5* μ.

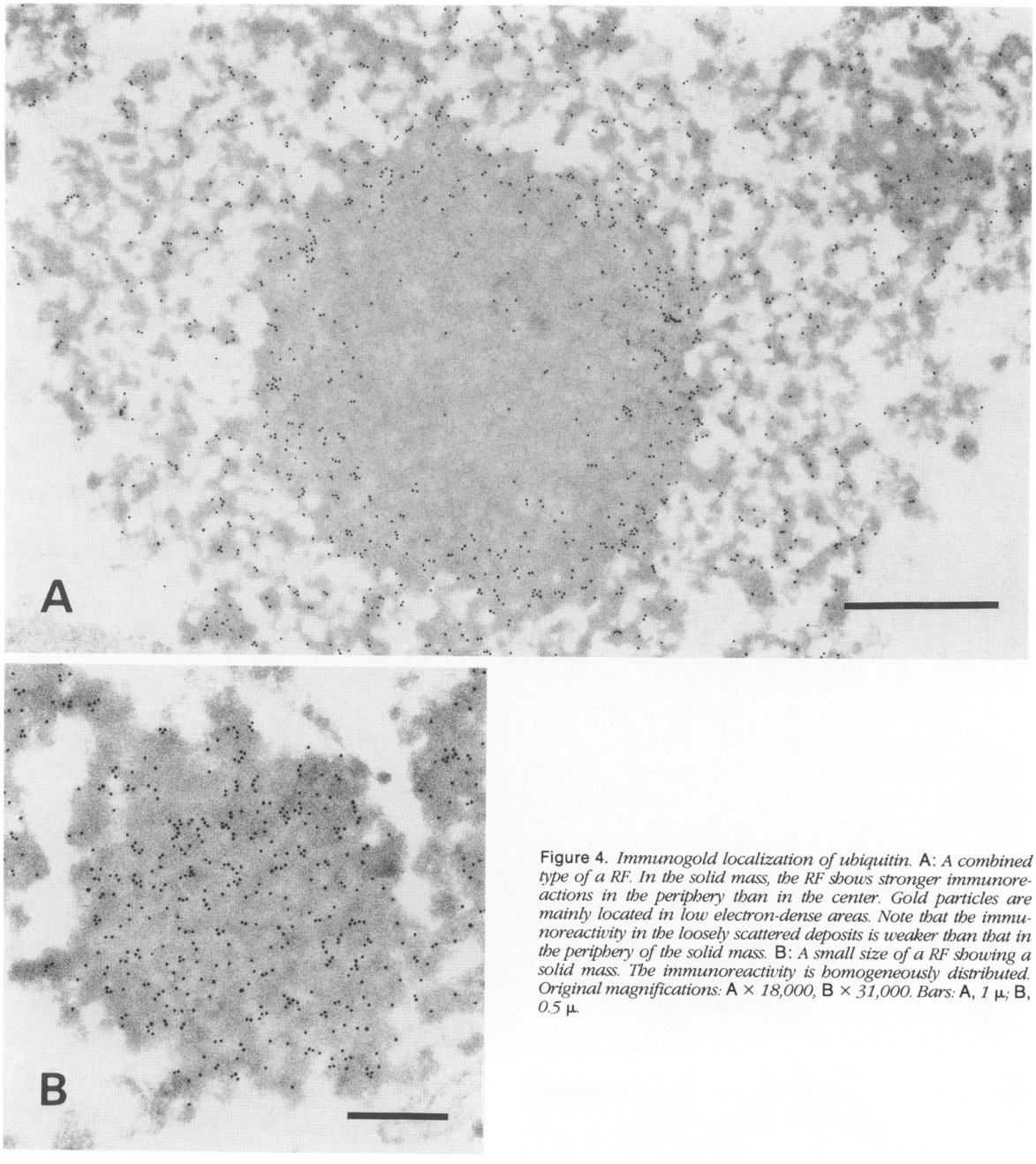

Figure 4. *Immunogold localization of ubiquitin.* A: *A combined type of a RF. In the solid mass, the RF shows stronger immunoreactions in the periphery than in the center. Gold particles are mainly located in low electron-dense areas. Note that the immunoreactivity in the loosely scattered deposits is weaker than that in the periphery of the solid mass.* B: *A small size of a RF showing a solid mass. The immunoreactivity is homogeneously distributed. Original magnifications:* A × *18,000,* B × *31,000. Bars:* A, *1* μ; B, *0.5* μ.

bovine-lens α-crystallin. (2) Substitution for the rabbit anti-αB-crystallin antiserum or the rabbit anti-GFAP antiserum by normal rabbit serum. (3) Omission of monoclonal antibodies.

Results

Morphologies of RFs

Rosenthal fibers isolated from an Alexander's disease brain showed irregular, amorphous, and electron-dense profiles, similar to that observed in formaldehyde-fixed, osmicated, and Epon-embedded tissue (Figures 1 to 6), and that previously described *in situ* in Alexander's disease[7,8,13–15] and in certain glial tumors.[10] Figure 1 showed in an Epon section a combined type of a RF both with a solid mass and with many loosely scattered deposits. This type of RFs was also detected in K4M section (Figures 2A, 4A). In the isolated RFs, the continuity of glial filaments with RFs was often disrupted at the margins. Individual RFs in K4M sections, in most cases, had a

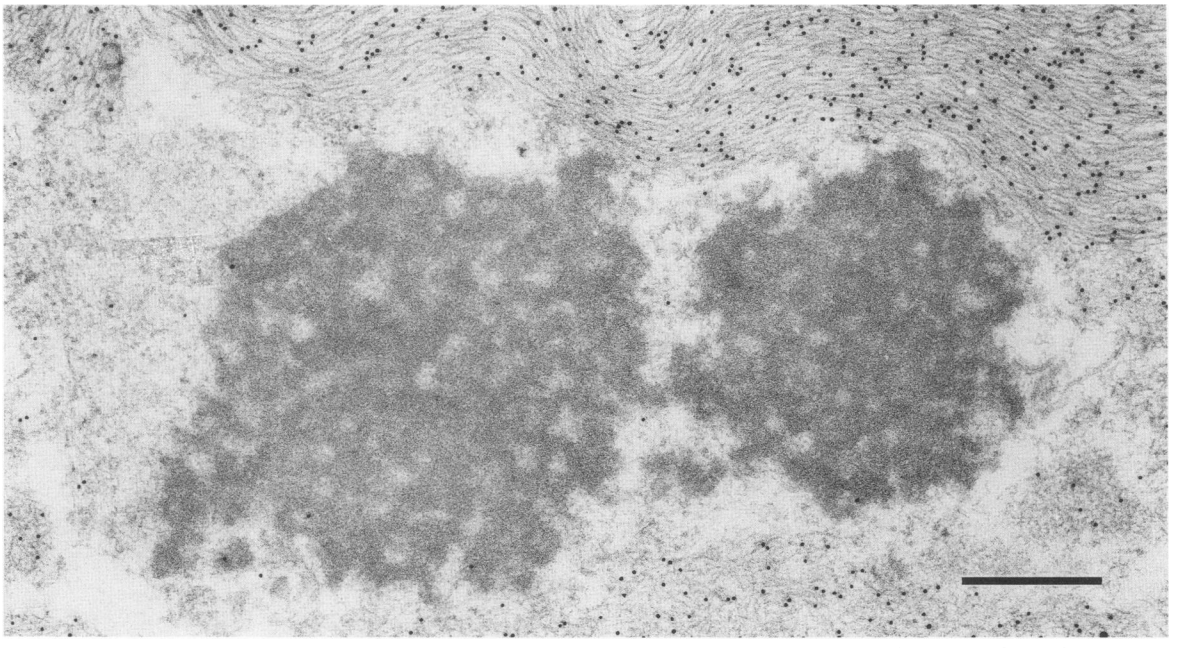

Figure 5. *Immunogold localization of vimentin. RFs are negative, although a few gold particles are seen in the margin of RFs. Filaments were heavily labeled. Original magnification × 37,000. Bar, 0.5 μ.*

heterogeneous electron density, especially when compared with the darker, more homogeneous appearance of RFs in tissue after osmication. Relatively high electron-dense areas were intermingled with lower electron-dense areas, where intermediate filaments could not be recognized. Particular attention was paid to the relationship between areas of different electron-densities and the immunoreactivities of αB-crystallin, GFAP, and ubiquitin.

Single Immunolabeling

αB-Crystallin

All RFs were immunolabeled with the anti–αB-crystallin antiserum (Figures 2A, B). Its labeling intensity was weak to strong and was not related to the diameter of RFs. In a combined type of RFs, immunoreactivity in the loosely scattered deposits was equivalent to or a little stronger than that in the solid mass of the center (Figure 2A). Among the variety of morphologies of RFs, loosely scattered deposits showed the highest density of gold particles (Figure 2A). In RFs showing a solid mass, most of the gold particles were found over high electron-dense areas (Figure 2B, Table 2). Bundles of intermediate filaments were occasionally labeled with a few gold particles (Figure 2A). RFs and filaments in control sections were not stained.

GFAP

All RFs were homogeneously and heavily labeled with both polyclonal and monoclonal anti-GFAP antibodies, including loosely scattered deposits (Figures 3A–C). Similar patterns of immunolabeling were obtained with both antibodies. GFAP immunoreactivity within RFs showing a solid mass was mainly localized in high electron-dense areas (Table 2). A dense feltwork of intermediate filaments also was heavily labeled with both antibodies.

Ubiquitin

Ubiquitin immunoreactivity was detected in most of the RFs observed. Its labeling pattern depended on the size of RFs. In large RFs showing a solid mass, the immunoreactions in the periphery were heavy but were reduced in the center (Figure 4A). In some large RFs, immunolabeling at the center was diminished severely or completely absent. In smaller RFs, the immunoreaction seemed to be homogeneous (Figure 4B). Although a few gold particles were located on high electron-dense area of RFs, most were observed on the low electron-dense areas, in contrast to αB-crystallin and GFAP (Table 2). Labeling density in loosely scattered deposits, in most cases, was lower than that in the periphery of RFs showing a solid mass (Figure 4A). Bundles of intermediate filaments were not stained.

Vimentin

In contrast to GFAP, no RFs were stained for vimentin, including loosely scattered deposits. Only a few gold particles were observed in the margin of some RFs. Interme-

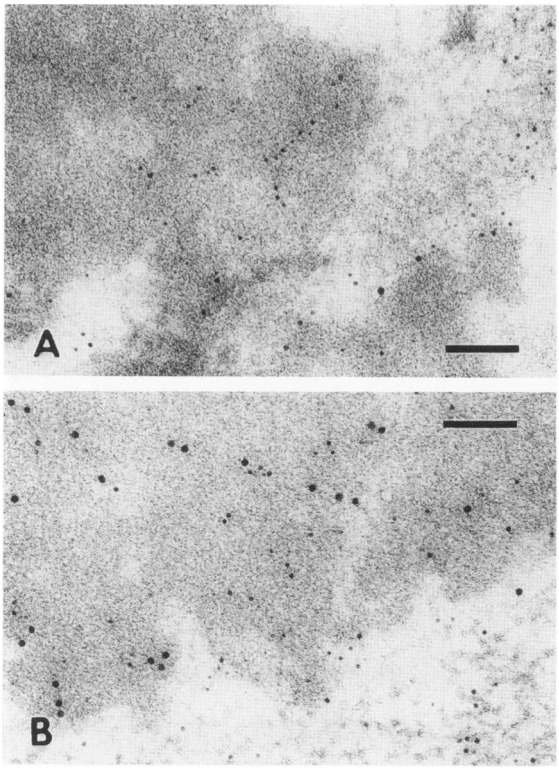

Figure 6. *Double immunolabeling of αB-crystallin and GFAP in a sequential double IGS. Severely decreased αB-crystallin immunoreactivity in a sequential double IGS with the first application of anti-GFAP antibody followed by the second application of anti-αB–crystallin antiserum* **(A)** *is noted when compared with that in a sequential double IGS with a reverse order of the antibodies* **(B)**. *Original magnifications × 98,000. Bars, 0.1 μ.*

diate filament bundles were labeled strongly with the anti-vimentin antibody, however (Figure 5).

Double Immunolabeling

In the sequential double IGS with the first application of a mouse anti-GFAP antibody followed by the second application of a rabbit anti–αB-crystallin antibody, αB-crystallin immunoreactivity was markedly reduced when compared with the sequential IGS with a reverse order of application of the primary antibodies (Figure 6A, B). In the simultaneous double IGS, the labeling intensity of αB-crystallin within RFs was low, similar to the level of the sequential double IGS with first application of GFAP antibody (Table 3). Double immunolabeling patterns of αB-crystallin and vimentin were simply combined patterns of each single staining either in simultaneous double IGS or in sequential double IGS.

Discussion

In this report we demonstrated immunoreactivities for αB-crystallin, GFAP, and ubiquitin in RFs using a low-temperature embedding procedure. Our procedures for immunoelectron microscopy have several advantages. First the frozen material still retained sufficient immunoreactivity and adequate fine structure despite the fact that the brain had been stored in a freezer at −35°C for 2 years. Second the isolation steps of RFs were simple and not time consuming. This technique should allow easy detection of RFs with various kinds of morphology because other cytoarchitectural components unnecessary for this study can largely be removed. Third the ultrastructural preservation of RFs embedded in Lowicryl K4M resin was equivalent to that obtained with epoxy resin. In general, embedding in hydrophilic resins at low temperature without osmication has been extremely favorable for obtaining good cytochemical labeling.[33] Because the cytoarchitecture of RFs seem to be stable against various kinds of experimental procedures, the postembedding IGS on Lowicryl K4M sections was selected for visualization of immunoreactivity of RFs.

Although immunogold localization of GFAP in the midst of RFs already was demonstrated in earlier studies,[18,19] the labeling intensity in this study was found to be much stronger than in the previous studies, perhaps because the use of hydrophilic resins containing 5% to 10% water and the omission of osmication can minimize the disruption of protein structure.[34] In fact, labeling density of gold particles in RFs was almost the same as that in a network of intermediate filaments. It is not known whether the GFAP associated with the matrix of RFs is the whole protein or degradation products thereof. If the latter is the case, then the breakdown products retain antigenic determinants recognized by these antibodies. At the light-microscopic level, GFAP immunoreactivity with RFs has been restricted to their periphery. This peripheral reaction was probably due to poor accessibility of epitopes within RFs. That is, the immunoreaction of GFAP probably occurs only on the surface or in superficial layers of RFs. The peripheral reactions probably result from a tangential view of immunostained products.

We first demonstrated ultrastructural immunogold localization of αB-crystallin in RFs. In double labeling for GFAP and αB-crystallin, we have consistently observed that the labeling density of immunogold became lower when a smaller size of gold (5 nm) was used in simultaneous double IGS. This indicates that molecules of αB-crystallin and GFAP are distributed close together on the accessible surface of RFs.

α-Crystallin is a major water-soluble lens protein of all vertebrate species. Its most striking characteristic is its enormous size, with aggregates of molecular weight close to 800 kd. These aggregates are produced by two homologous, highly conserved genes (αA and αB), which encode subunits of about 20 kd.[35] The αA-crystallin gene appears to be expressed specifically in the lens.[36] In contrast, αB-crystallin is found in many

Table 2. *Distributions of Gold Particles in High and Low Electron-Dense Areas of Rosenthal Fibers*

Antibody		% of gold particles	
		High electron dense	Low electron dense
αB-crystallin	(11)	72.8 ± 4.2	18.6 ± 5.1
GFAP	(10)	75.5 ± 4.7	12.2 ± 6.2
Ubiquitin	(10)	23.9 ± 6.4	61.3 ± 5.6

The ratios of number of gold particles located on high or low electron-dense area to total number of gold particles in each RF were averaged. Gold particles on the transitional zones between high and low electron-dense areas were counted only into total number of gold. Values are expressed as the mean ± SD. Values in parentheses are the number of RFs counted.

extralenticular tissues, including heart, muscle, kidney, and brain, by immunohistochemistry and by Western and Northern blotting.[17,24–27] The nature of α-crystallin was investigated extensively, especially from the point of view of cataract formation.[37,38] In the lens, α-crystallin is contained in both water-soluble and water-insoluble fractions, suggesting the associations between α-crystallin and cytoskeletal or membrane components.[38] High–molecular-weight (HMW) aggregates containing α-crystallin were also detected in the soluble fraction.[38] In another report, it was observed that the aggregation of α-crystallin was induced by the addition of nonlens protein to concentrated α-crystallin probably by an excluded volume effect and was inhibited by γ-crystallin enriched with exposed thiols.[39] This HMW aggregate, the cause of which is still unknown, is certain to be related to the self-aggregating nature of α-crystallin. In extralenticular tissues, soluble αB-crystallin exists in an aggregate form with molecular weight indistinguishable from that of lens α-crystallin, and the presence of the αA-crystallin is not required to form these aggregates.[40] Post-translational modifications also may play a role in aggregation.[35,37]

The present observations support the idea that RFs are in part aggregation products of αB-crystallin.[24] A possible scheme for their morphogenesis is as follows: astrocytes under certain pathologic conditions, such as Alexander's disease, accumulate αB-crystallin. The expression of αB-crystallin in reactive astrocytes supports the idea that the nonlens role of αB-crystallin may be connected to its ancestral relationship with small heat shock proteins.[41] Accumulation of αB-crystallin may facilitate the enormous aggregate state, by which chemical nature of αB-crystallin is well known in the lens.[38] The massive accumulation of glial filaments could facilitate the self-aggregation of αB-crystallin, probably by their volume effect.[39] This initial abnormal HMW of αB-crystallin possibly is loosely scattered deposits as shown in Figures 1, 2A, 3C, and 4A. During the initial stage of RFs, GFAP in glial filaments may be involved without degradation. The RFs may expand their volumes by involving marginal, small RFs. The chemical alteration of αB-crystallin during RF formation is not known. In view of insoluble HMW aggregates of α-crystallin subject to post-translational modifications in cataract,[38] however, αB-crystallin also is probably subject to similar post-translational modifications during RF formation.

Table 3. *Alterations of Immunoreactivities of αB-crystallin Among Three Double-immunostaining Methods*

		% of gold particles
Sequential double IGS		
αB-crystallin → GFAP	(12)	38.2 ± 4.3†
GFAP → αB-crystallin	(10)	9.5 ± 3.3*
Simultaneous double IGS	(10)	12.6 ± 3.5*

The ratio of a number of gold particles indicating αB-crystallin immunoreactivity to the total number of gold particles was calculated in each RF and was averaged. Values are expressed as the mean ± SD. Figures in parentheses are the number of RFs counted.
* Statistically significant compared with the value† ($P < 0.01$)

Ubiquitination might be a secondary reaction. In the center of the large RFs, ubiquitin immunoreactivity was weak or absent (Figure 4A). It is uncertain whether there is a loss of ubiquitin immunoreactivity in the center or only a lesser amount of ubiquitin can infiltrate deep into the center. It was reported that both anti-ubiquitin antibody and anti-GFAP antibody immunolabeled mainly the periphery of RFs at the light-microscopic level, and that RFs were based on the ubiquitination of glial filaments.[21] At the electron-microscopic level, however, distribution of ubiquitin immunoreactivity (Figure 4A) did not correspond to those of GFAP (Figures 3A, B) and αB-crystallin (Figures 2A, B). Recently proteins with acetylated NH_2-termini, including αA-crystallin, were also found to be degraded in a ubiquitin-dependent mode *in vitro* reticulocyte system.[42] Therefore further biochemical investigation is needed to identify target proteins for ubiquitination in RFs.

Interestingly vimentin, a component protein of intermediate filament, was not detected in RFs. The discrepancy in RFs between GFAP and vimentin is difficult to explain. It is possible that degradation products of vimentin, not recognized by the antibody, are present or, alternatively, that the vimentin in the crude preparation[17,24] comes only from filaments. Further study is needed to resolve the difference in biochemical function between those two intermediate proteins, especially in terms of their interactions with αB-crystallin.

In conclusion, we show at electron-microscopic level that; 1) RFs share epitopes with αB-crystallin, GFAP, and ubiquitin, but not with vimentin; and 2) immunolabeling

patterns of gold probes are indicative of the heterogeneous chemical structure of RFs.

Acknowledgments

The authors thank Professor T. Kosaka and Dr. Y. Sato for their technical advice in immunoelectron microscopy.

References

1. Rosenthal W: Ueber eine eigenthmliche, mit Syringomyelie complicirte Geschwulst des Rckenmarks. Beitr Path Anat 1898, 23:111–143
2. Alexander WS: Progressive fibrinoid degeneration of fibrillary astrocytes associated with mental retardation in a hydrocephalic infant. Brain 1949, 72:373–381
3. Crome L: Megalencephaly associated with hyaline panneuropathy. Brain 1953, 76:215–228
4. Grcevic N, Yates PO: Rosenthal fibers in tumours of the central nervous system. J Pathol Bacteriol 1957, 73:467–472
5. Vogel FS, Hallervorden J: Leukodystrophy with diffuse Rosenthal fiber formation. Acta Neuropathol (Berl) 1962, 2:126–143
6. Friede RL: Alexander's disease. Arch Neurol 1964, 11:414–422
7. Seil FJ, Schochet SS, Earle KM: Alexander's disease in adult: Report of a case. Arch Neurol 1968, 19:494–502
8. Herndon RM, Rubinstein LJ, Freeman JM, Mathieson G: Light and electron microscopic observations on Rosenthal fibers in Alexander's disease and in multiple sclerosis. J Neuropathol Exp Neurol 1970, 29:524–551
9. Tihen WS: Central pontine myelinolysis and Rosenthal fibers of the brainstem. Association with emaciation and prolonged intravenous hyperalimentation. Neurology 1972, 22:710–716
10. Gullotta F, Fliedner E: Spongioblastomas, astrocytomas, and Rosenthal fibers. Ultrastructural, tissue culture and enzyme histochemical investigations. Acta Neuropathol (Berl) 1972, 22:68–78.
11. Russo LS, Aron A, Anderson PJ: Alexander's disease: A report and reappraisal. Neurology 1976, 26:607–614
12. Kress Y, Gaskin F, Horoupian DS, Brosnan C: Nickel induction of Rosenthal fibers in rat brain. Brain Res 1981, 210:419–425
13. Towfighi J, Young R, Sassani J, Ramer J, Horoupian DS: Alexander's disease: Further light-, and electron-microscopic observations. Acta Neuropathol (Berl) 1983, 61:36–42
14. Walls TJ, Jones RA, Cartlidge N, Saunders M: Alexander's disease with Rosenthal fibre formation in an adult. J Neurol Neurosurg Psychiatry 1984, 47:399–403
15. Borrett D, Becker LE: Alexander's disease. A disease of astrocytes. Brain 1985, 108:367–385
16. Janzer RC, Friede RL: Do Rosenthal fibers contain glial fibrillary acid protein? Acta Neuropathol (Berl) 1981, 55:75–76
17. Goldman JE, Corbin E: Isolation of a major protein component of Rosenthal fibers. Am J Pathol 1988, 130:569–578
18. Dinda AK, Sarkar C, Roy S: Rosenthal fibers: An immunohistochemical, ultrastructural and immunoelectron microscopic study. Acta Neuropathol (Berl) 1990, 79:456–460
19. Bettica A, Johnson AB: Ultrastructural immunogold labeling of glial filaments in osmicated and unosmicated epoxy-embedded tissue. J Histochem Cytochem 1990, 38:103–109
20. Lowe J, Blanchard A, Morrell K, Lennox G, Reynolds L, Billett M, Landon M, Mayer J: Ubiquitin is a common factor in intermediate filament inclusion bodies of diverse type in man, including those of Parkinson's disease, Pick's disease, and Alzheimer's disease, as well as Rosenthal fibers in cerebellar astrocytomas, cytoplasmic bodies in muscle, and Mallory bodies in alcoholic liver disease. J Pathol 1988, 155:9–15
21. Lowe J, Morrell K, Lennox G, Landon M, Mayer RJ: Rosenthal fibres are based on the ubiquitination of glial filaments. Neuropathol Appl Neurobiol 1989, 15:45–53
22. Hershko A, Eytan E, Ciechanover A: Immunochemical analysis of the turnover of ubiquitin-protein conjugates in intact cells. Relationship to the breakdown of abnormal proteins. J Biol Chem 1982, 257:13964–13970
23. Manetto V, Perry G, Tabaton M, Mulvihill P, Fried VA, Smith HT, Gambetti P, Autillo-Gambetti L: Ubiquitin is associated with abnormal cytoplasmic filaments characteristic of neurodegenerative diseases. Proc Natl Acad Sci USA 1988, 85:4501–4505
24. Iwaki T, Kume-Iwaki A, Liem RKH, Goldman JE: αB-crystallin is expressed in non-lenticular tissues and accumulates in Alexander's disease brain. Cell 1989, 57:71–78
25. Iwaki T, Kume-Iwaki A, Goldman JE: Cellular distribution of αB-crystallin in non-lenticullar tissues. J Histochem Cytochem 1990, 38:31–39
26. Bhat SP, Nagineni CN: αB subunit of lens-specific protein α-crystallin is present in other ocular and non-ocular tissues. BBRC 1989, 158:319–325
27. Dubin RA, Wawrousek EF, Piatigorsky J: Expression of the murine αB-crystallin gene is not restricted to the lens. Mol Cell Biol 1989, 9:1083–1091
28. Altman LG, Schneider BG, Papermaster DS: Rapid embedding of tissues in Lowicryl K4M for immunoelectron microscopy. J Histochem Cytochem 1984, 32:1217–1223
29. Goldman JE, Chiu FC: Growth kinetics, cell shape, and the cytoskeleton of primary astrocyte cultures. J Neurochem 1984, 42:175–184
30. Debus E, Weber K, Osborn M: Monoclonal antibodies specific for glial fibrillary acidic protein and for each of the neurofilament triplet polypeptides. Differentiation 1983, 25:193–203
31. Haas AL, Bright PM: The immunohistochemical detection

and quantitation of intracellular ubiquitin-protein conjugates. J Biol Chem 1985, 260:12464–12473

32. Osborn M, Debus E, Weber K: Monoclonal antibodies specific for vimentin. Eur J Cell Biol 1984, 34:137–143
33. Roth J, Bendayan M, Carlemalm E, Villiger W, Garavito M: Enhancement of structural preservation and immunocytochemical staining in low temperature embedded pancreatic tissue. J Histochem Cytochem 1981, 29:663–671
34. Newman GR, Jasani B, Williams ED: A simple post-embedding system for the rapid demonstration of tissue antigens under the electron microscope. Histochem J 1983, 15:543–555
35. Wistow GJ, Piatigorsky J: Lens crystallins: The evolution and expression of proteins for a highly specialized tissue. Annu Rev Biochem 1988, 57:479–504
36. Overbeek PA, Chepelinsky AB, Khillan JS, Piatigorsky J, Westphal H: Lens-specific expression and developmental regulation of the bacterial chloramphenical acetyltransferase gene driven by the murine αA-crystallin promotor in transgenic mice. Proc Natl Acad Sci USA 1985, 82:7815–7819
37. Bleomendal H: The vertebrate eye lens. A useful system for the study of fundamental biological processes on a molecular level. Science 1977, 197:127–138
38. Harding JJ: Changes in lens proteins in cataract, Molecular and Cellular Biology of the Eye Lens. Edited by Bleomendal H. New York, John Wiley & Sons, 1981, pp 327–365
39. Mach H, Trautman PA, Thomson JA, Lewis RV, Middaugh CR: Inhibition of α-crystallin aggregation by γ-crystallin. J Biol Chem 1990, 265:4844–4848
40. Chiesa R, McDermott MJ, Mann E, Spector A: The apparent molecular size of native α-crystallin B in non-lenticular tissues. FEBS Lett 1990, 268:222–226
41. Ingolia TD, Craig EA: Four small *Dorsophila* heat shock proteins are related to each other and to mammalian α-crystallin. Proc Natl Acad Sci USA 1982, 79:2360–2364
42. Mayer A, Siegel NR, Schwartz AL, Ciechanover A: Degradation of proteins with acetylated amino termini by ubiquitin system. Science 1989, 244:1480–1483